arXiv:1403.5205v1 [quant-ph] 20 Mar 2014

Quantum walks on a circle with optomechanical systems

J. K. Moqadam,[1] R. Portugal,[1] and M. C. de Oliveira[2,*]

[1]*Laboratório Nacional de Computação Científica (LNCC), Petrópolis, RJ, Brazil*
[2]*Instituto de Física "Gleb Wataghin", Universidade Estadual de Campinas, 13083-970, Campinas, SP, Brazil*

(Dated: March 21, 2014)

We propose an implementation of a quantum walk on a circle on an optomechanical system by encoding the walker on the phase space of a radiation field and the coin on a two-level state of a mechanical resonator. The dynamics of the system is obtained by applying Suzuki-Trotter decomposition. We numerically show that the system displays a typical behavior of quantum walks, namely, the probability distribution evolves ballistically and the standard deviation of the phase distribution is linearly proportional to the number of steps. We also analyze the effects of decoherence by using the phase damping channel on the coin space, showing the possibility to implement the quantum walk with present day technology.

PACS numbers: 03.67.Ac,05.40.fb,07.10.Cm,42.50.Wk

I. INTRODUCTION

Discrete time quantum walks are the counterpart of the classical random walks when the coin used to direct the walker steps can assume a superposition of its possible states [1]. This ability to exist in a superposition leads to a highly entangled joint state for the coin and walker over time [2], resulting in a clear speedup. Therefore it is not surprising that similarly to its classical version, quantum walks are connected to the success of search algorithms, depending on the pertinent geometry [3, 4]. This success has promoted a broad investigation over the last years, from computational (algorithmic) point of view [5] or in order to efficiently implement it physically [6]. Actual implementations were reported through experiments on optical [7–14] and atomic systems [15–18].

Particularly interesting from the quantum optics perspective is the quantum walk on a circle since it can be implemented on a large number of systems, with a variable amount of control. The general idea is that the walker steps are encoded as phase increments in the phase space of a harmonic oscillator, whose signal is conditioned to an auxiliary quantum coin. Some examples of systems explored include micromasers [1], optical lattices [19], ion traps [20], cavity quantum electrodynamics [21, 22], as well as in superconducting circuit quantum electrodynamics [23]. A natural system where the quantum walk on a circle can be implemented though is on the emerging field of quantum optomechanics, where quantum mechanical modes can be coupled to quantum light modes [24]. Given the degree of control achieved and the ability to reach an enormous variety of strong coupling in those systems [25], a particular advantage over the previous experimental realizations would be the possibility to implement a quantum walk on a large number of time steps. It is therefore expected that they might be employed in the near future for implementation of a quantum walk, be it on the optical or the microwave regime.

Here we propose an implementation of a quantum walk on a circle in an optomechanical (or electromechanical) system. The proposed system is an optomechanical resonator, which is composed of an optical cavity coupled to a mechanical resonator as presented in Fig. 1(a). This kind of system has been explored in many physical experiments [24], and the quantum regime has been recently reached [25–28]. We assume a dispersive interaction between the mechanical mode and the radiation, which that can in principle be achieved in both optical and microwave regimes due to radiation pressure [28]. This interaction provides a way to implement the operations employed in quantum walks. The position of a coherent state in the phase space for the radiation mode is used to encode the position of the walker, while the mechanical mode plays the role of a quantum coin.

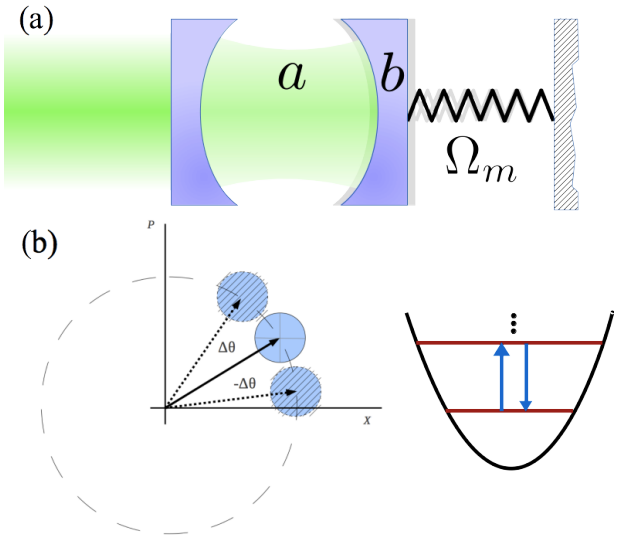

FIG. 1. (Color Online) Quantum walk implemented with a typical quantum optomechanical system (a) where a radiation mode a is coupled to a mechanical mode of frequency Ω_m. (b) The optical field described by a coherent state has its phase shifted by $\Delta\theta$ or $-\Delta\theta$ conditioned on the state of the quantum coin encoded in the two lowest levels of the mechanical mode.

We investigate the situation for a two-sided coin by considering low excitation of the mechanical resonator, where it can be appropriately described by a two-level system. The shift

* marcos@ifi.unicamp.br

operator is implemented via the coupling to the mechanical resonator. By adjusting the frequency, its evolution is driven by a Hadamard-like operator, necessary in the evolution. By performing numerical simulations, we show that the dynamics of the system present the main signature of the quantum walk evolution, namely, the ballistic spread of the phase probability distribution. The transition from quantum to classical walk due to noise effects on the coin is investigated by introducing decoherence via the phase damping channel on the coin space.

The paper is structured as follows. In Sec. II we derive the dynamics of the systems and describe how the coined quantum walk can be implemented. In Sec. III we analyze the decoherence by using the phase damping channel affecting the coin. Finally, the summary and discussion are presented in Sec. IV.

II. QUANTUM WALK IN PHASE SPACE OF AN OPTICAL RESONATOR

The optomechanical Hamiltonian in a frame rotating with the drive frequency is given by [24]

$$\begin{aligned}\mathcal{H} =& -\hbar\Delta a^\dagger a + \hbar\Omega_m b^\dagger b - \hbar g_0 a^\dagger a(b^\dagger + b) \\ &+ \hbar\varepsilon(a^\dagger + a),\end{aligned} \tag{1}$$

where $a^\dagger$ (a), $b^\dagger$ (b) are the creation (annihilation) operators for the optical and mechanical resonators respectively, Δ is the drive field detuning with respect to the cavity resonance mode, Ω_m is the mechanical resonator frequency, g_0 is the photon-phonon interaction strength, which is given due to radiation pressure force, and ε is the drive amplitude.

In a stationary regime the driving ε competes with dissipative effects (described by an amplitude damping channel at $T = 0$) forcing the optical field to be in a coherent state, a state with a well defined phase [see Fig. 1(b)]. The coupling considered induces a frequency shift on the optical field conditioned on the displacement of the mechanical resonator. Since the optical field is in a coherent state, the frequency shift translates into a wandering of the optical field phase conditioned on the excitations of the mechanical resonator. Consider for example the action of the evolution operator due to the interaction Hamiltonian only. If the optical mode is in a coherent state $|\alpha\rangle$ and the mechanical mode in a position eigenstate $|x\rangle$ then

$$e^{i\ g_0 t a^\dagger a(b+b^\dagger)}|\alpha\rangle|x\rangle = |\alpha e^{i\ g_0' x t}\rangle|x\rangle,$$

with $g_0' = g_0\sqrt{2m\Omega_m/\hbar}$. If $x = x_0 \pm \Delta x$, being x_0 the equilibrium position for the mechanical resonator and Δx its maximal displacement, then

$$e^{i\ g_0 t a^\dagger a(b+b^\dagger)}|\alpha\rangle|x_0 \pm \Delta x\rangle = |\alpha e^{i\ g_0' t(x_0 \pm \Delta x)}\rangle|x_0 \pm \Delta x\rangle,$$

and the mechanical resonator induces a phase shift $\pm g_0' t\Delta x$ on the coherent state of the optical mode conditioned on the displacement $\pm\Delta x$. This feature clearly suggests that the coupling should be explored as the shift operator in the standard quantum walk. This is best appreciated if we consider the situation where the mechanical resonator is cooled down to its ground state [25–28] and from there can be coherently promoted to the first excited state, such that, the average number of phonons, $\langle b^\dagger b\rangle < 1$. The mechanical resonator can therefore be approximately described by only its two lowest energy levels and its creation and annihilation operators are replaced, respectively, by the spin raising and lowering operators $\sigma_+ = |e\rangle\langle g|$ and $\sigma_- = |g\rangle\langle e|$, where $|g\rangle$ and $|e\rangle$ are the ground and the first exited states of the mechanical resonator, constituting a two-sided quantum coin. Relations $\sigma_+\sigma_- = (1/2)(I + \sigma_z)$ and $\sigma_+ + \sigma_- = \sigma_x$ can then be used where by performing a basis change to the rotated frame $|\pm\rangle = (1/\sqrt{2})(|e\rangle \pm |g\rangle)$, Pauli matrices σ_x and σ_z are replaced by $\tilde{\sigma}_z$ and $\tilde{\sigma}_x$, respectively. Neglecting the constant energy, the Hamiltonian (1) can be rewritten as

$$\mathcal{H} = -\hbar\Delta a^\dagger a - \hbar g_0 a^\dagger a\tilde{\sigma}_z + \hbar\varepsilon(a^\dagger + a) + \frac{1}{2}\hbar\Omega_m\tilde{\sigma}_x. \tag{2}$$

Using the Suzuki-Trotter formula [29] we can express the evolution operator, given the Hamiltonian (2) as

$$\begin{aligned}\mathcal{U}(T) &= e^{-i\mathcal{H}t/\hbar} \\ &= \lim_{n\to\infty}\{e^{iT\Delta a^\dagger a/n}\cdot e^{iTg_0 a^\dagger a\tilde{\sigma}_z/n}\cdot \\ &\qquad e^{-iT\varepsilon(a^\dagger+a)/n}\cdot e^{-iT\Omega_m\tilde{\sigma}_x/(2n)}\}^n,\end{aligned} \tag{3}$$

where T is the total time evolution and n is the number of total time partitions. Generally for any set of skew-Hermitian operators $\{H_j; j = 1, ..., p\}$ in a Banach space, the first order Suzuki-Trotter approximation error ϵ is bounded as [29, 30]

$$\begin{aligned}\left\|\exp\left(\sum_{j=1}^{p} H_j\right) - \left[\prod_{j=1}^{p}\exp\left(\frac{1}{n}H_j\right)\right]^n\right\| \\ \leq \frac{1}{2n}\sum_{j>k}\|[H_j, H_k]\|.\end{aligned} \tag{4}$$

Actually, the limit in Eq. (3) is a result of Eq. (4) provided that the operators are bounded. It must be mentioned that the annihilation and creation operators $a^\dagger$ and a are not bounded in general. However, they remain bounded when restricted to operate on the coherent states with bounded displacement of the vacuum state.

The upper bound error corresponding to Eq. (4) for a finite n is then calculated as

$$\begin{aligned}\epsilon \leq \frac{T^2}{2n}\Big(&\Delta\varepsilon\|a^\dagger - a\| + \Omega_m g_0\|\tilde{\sigma}_y a^\dagger a\| \\ &+ g_0\varepsilon\|\tilde{\sigma}_z(a^\dagger - a)\|\Big).\end{aligned} \tag{5}$$

Using the operator norm

$$\|H_j\| := \sup_{\||\psi\rangle\|=1}\|H_j|\psi\rangle\|,$$

with $|\psi\rangle = |q\rangle|\alpha\rangle$, where $|q\rangle$ is the state of the qubit and $|\alpha\rangle$ is the coherent state of the optical field, the error can be written

as

$$\epsilon \leq \frac{T^2}{2n}\Big[\varepsilon(\Delta+g_0)\left(|\alpha_{\max}|+\sqrt{1+|\alpha_{\max}|^2}\right) + \Omega_m g_0|\alpha_{\max}|\sqrt{1+|\alpha_{\max}|^2}\Big], \quad (6)$$

where $\alpha_{\max}$ has the largest modulus over the whole desired (bounded) region of the phase space. Therefore, by taking n sufficiently large the error can be made as small as required.

A. Quantum walk dynamics

Taking n large enough as discussed above and choosing the mechanical resonator frequency so that

$$\tau \equiv \frac{T}{n} = \frac{\pi}{2\Omega_m}, \quad (7)$$

the approximate evolution of the system is given by

$$\mathcal{U}(T) \approx \mathcal{U}_{ST}(n\tau) = U^n, \quad (8)$$

where

$$U = e^{i\tau\Delta a^\dagger a}e^{i\tau g_0 a^\dagger a\tilde{\sigma}_z}e^{-i\tau\varepsilon(a^\dagger+a)}e^{-i\frac{\pi}{4}\tilde{\sigma}_x}. \quad (9)$$

The evolution (8) corresponds to a n-step discrete-time quantum walk when $\tau\varepsilon$ is small. The state of the quantum walk is the product of the mechanical resonator 2-level state with the coherent state of the optical field. The coherent state is conditionally shifted depending on the state of the qubit. Specifically, the last term in r.h.s. of Eq. (9) can generate a Hadamard-like transformation for the qubit since

$$e^{-i\frac{\pi}{4}\tilde{\sigma}_x} = \frac{1}{\sqrt{2}}\begin{pmatrix}1 & -i\\ -i & 1\end{pmatrix} = \frac{1}{\sqrt{2}}\begin{pmatrix}1 & 0\\ 0 & -i\end{pmatrix}\begin{pmatrix}1 & 1\\ 1 & -1\end{pmatrix}\begin{pmatrix}1 & 0\\ 0 & -i\end{pmatrix}. \quad (10)$$

This term plays the role of the coin operator.

The coherent state of the optical resonator

$$|\alpha\rangle = e^{-\frac{1}{2}|\alpha|^2}\sum_{j=0}^{\infty}\frac{\alpha^j}{\sqrt{j!}}|j\rangle, \quad (11)$$

where $|j\rangle$ are the number states of the resonator, is rotated in the phase space, as in Fig. 1(b) for $\Delta\theta = \tau g_0$ under the application of the second term in Eq. (9)

$$e^{i\tau g_0 a^\dagger a\tilde{\sigma}_z}|\alpha\rangle|\pm\rangle = |\alpha e^{\pm i\tau g_0}\rangle|\pm\rangle, \quad (12)$$

conditioned on the coin state $|\pm\rangle$. This last term plays the role of the shift operator [20, 23].

The third term in Eq. (9) disturbs the quantum walk dynamics, but it can be made small enough in order to keep the quantum walk characteristics. Finally, the first term is a free rotation that is not related with the shift operator (second term). Its effect is an overall phase shift. The effects of the first and third terms are also discussed later.

It is now possible to find the dynamics of the system during the time $T = n\tau$. Starting with the initial state

$$|\psi_0\rangle = |+\rangle|\alpha_0\rangle, \quad (13)$$

after the first time step the system evolves to

$$|\psi_1\rangle = U|+\rangle|\alpha_0\rangle,$$

which can be eventually simplified to

$$|\psi_1\rangle = c_1^{(1)}|+\rangle|\alpha_1^{(1)}\rangle + c_2^{(1)}|-\rangle|\alpha_2^{(1)}\rangle, \quad (14)$$

where

$$\begin{cases}\alpha_1^{(1)} = (\alpha_0 - i\tau\varepsilon)e^{i\tau(\Delta+g_0)},\\ \alpha_2^{(1)} = (\alpha_0 - i\tau\varepsilon)e^{i\tau(\Delta-g_0)},\end{cases} \quad (15)$$

and

$$\begin{cases}c_1^{(1)} = \frac{1}{\sqrt{2}}e^{-i\tau\varepsilon\mathrm{Re}(\alpha_0)},\\ c_2^{(1)} = \frac{-i}{\sqrt{2}}e^{-i\tau\varepsilon\mathrm{Re}(\alpha_0)}.\end{cases} \quad (16)$$

In the same way it is possible to calculate the state of the system in the next time steps. In each time step the number of terms is twice the number of terms in the previous state. Associating the odd subindices to the terms with $|+\rangle$ and the even subindices to the terms with $|-\rangle$ in all time steps, the state of the system at step l can be written as

$$|\psi_l\rangle = \sum_{k=1}^{2^{l-1}}\left\{c_{2k-1}^{(l)}|+\rangle|\alpha_{2k-1}^{(l)}\rangle + c_{2k}^{(l)}|-\rangle|\alpha_{2k}^{(l)}\rangle\right\}, \quad (17)$$

where $1 \leq l \leq n$. Recursively, the complex numbers α are obtained as

$$\begin{cases}\alpha_{2k-1}^{(l)} &= [\alpha_k^{(l-1)} - i\tau\varepsilon]e^{i\tau(\Delta+g_0)},\\ \alpha_{2k}^{(l)} &= [\alpha_k^{(l-1)} - i\tau\varepsilon]e^{i\tau(\Delta-g_0)},\end{cases} \quad (18)$$

for $l \geq 2$ with the initial condition given by Eq. (15). For odd k, coefficients c are calculated as

$$\begin{cases}c_{2k-1}^{(l)} &= (\frac{1}{\sqrt{2}})^l c_k^{(l-1)}e^{-i\tau\varepsilon\mathrm{Re}[\alpha_k^{(l-1)}]},\\ c_{2k}^{(l)} &= (\frac{-i}{\sqrt{2}})^l c_k^{(l-1)}e^{-i\tau\varepsilon\mathrm{Re}[\alpha_k^{(l-1)}]},\end{cases} \quad (19)$$

and for even k,

$$\begin{cases}c_{2k-1}^{(l)} &= (\frac{-i}{\sqrt{2}})^l c_k^{(l-1)}e^{-i\tau\varepsilon\mathrm{Re}[\alpha_k^{(l-1)}]},\\ c_{2k}^{(l)} &= (\frac{1}{\sqrt{2}})^l c_k^{(l-1)}e^{-i\tau\varepsilon\mathrm{Re}[\alpha_k^{(l-1)}]},\end{cases} \quad (20)$$

for $l \geq 2$ with the initial condition given by Eq. (16).

The characteristics of the quantum walk dynamics are revealed when looking at the phase probability distribution of state (17) in the phase space. The coherent state $|\alpha_k\rangle$ rotates by an angle $\pm\Delta\theta = \pm\tau g_0$ in each time step [see Eq. (12)]

which leads to a set of discrete angles in the phase space [see Fig. 1(b)]. The Hilbert space for the quantum walk is

$$\mathrm{H}_d = \mathrm{span}\Big\{|\varphi_m = \frac{2\pi m}{d}\rangle = \frac{1}{\sqrt{d}}\sum_{j=0}^{d-1} e^{ij\varphi_m}|j\rangle; \quad m = 0, 1, \ldots, d-1\Big\}, \tag{21}$$

where $|\varphi_m\rangle$ are known as the phase states [31] and play the role of the computational basis. Here, d is the Hilbert space dimension which is set to $2\pi/(\tau g_0)$. The projection of the system state (17) into H_d is given by

$$|\psi_l\rangle_d = \sum_{k=1}^{2^{l-1}}\sum_{m=1}^{d-1}\Big\{c^{(l)}_{2k-1}\langle\varphi_m|\alpha^{(l)}_{2k-1}\rangle|+\rangle|\varphi_m\rangle + c^{(l)}_{2k}\langle\varphi_m|\alpha^{(l)}_{2k}\rangle|-\rangle|\varphi_m\rangle\Big\}. \tag{22}$$

All coherent states in Eq. (22) are truncated when projected into H_d, because d is finite. However, if $d > |\alpha|^2 + |\alpha|$, where $|\alpha|^2$ represents the average number of photons in the coherent state and $|\alpha|$ is the corresponding standard deviation, the projection of the coherent state $|\alpha\rangle$ onto Hilbert space H_d will be an acceptable approximation for $|\alpha\rangle$ [21]. Moreover, since the coherent states have a minimum uncertainty of $1/2$ [31], the value of d cannot be arbitrarily large. In fact, in a circle of radius $|\alpha|$ at most $4\pi|\alpha|$ distinguishable coherent states can be fitted. Therefore, the condition $d \leq 4\pi|\alpha|$ must be imposed. By equating the lower and the upper bounds for d we obtain that $|\alpha| = 4\pi - 1$. We conclude that the upper bound for the number of sites in the circle is around 145 (a cycle with 145 vertices).

Using Eq. (22), the (unnormalized) probability distribution of the walker in the phase space is calculated as

$$P^{(l)}(m) = \left|\Big(\langle+|\langle\varphi_m|\Big)|\psi_l\rangle\right|^2 + \left|\Big(\langle-|\langle\varphi_m|\Big)|\psi_l\rangle\right|^2, \tag{23}$$

where the expression

$$\langle\varphi_m|\alpha^{(l)}_k\rangle = \frac{1}{\sqrt{d}}e^{-\frac{1}{2}\left|\alpha^{(l)}_k\right|^2}\sum_{j=0}^{d-1}\frac{\left(\alpha^{(l)}_k e^{-i\varphi_m}\right)^j}{\sqrt{j!}}, \tag{24}$$

for $k = 1, \ldots 2^l$ is used in order to calculate $\langle\varphi_m|\psi_l\rangle$. In the next section it is discussed how to normalize $P^{(l)}(m)$.

Figure 2 shows $P^{(l)}(m)$ for some values of l taking (13) as initial state. Step $l = 0$ corresponds to the initial distribution. The figure helps to see some characteristics of the quantum walk propagation, which are remarkably different from classical random walks. The probability distribution of quantum walks can have high peaks far from the origin, while random walks are described by normal distributions.

To further stress the difference between quantum walks and random walks, we analyze the dependence of the phase standard deviation (σ) as a function of time steps (l). It is well known that $\sigma \propto \sqrt{l}$ for random walks. Figure 3 shows σ as a function of l for two initial states obtained from our simulations. Clearly, there is a linear dependence or a ballistic behavior for both initial states. The black line ($\times$ points) can be approximately expressed as $\sigma \approx 0.45\,l + 0.77$, which uses initial state (13). The blue line ($+$ points) can be approximately expressed as $\sigma \approx 0.56\,l + 0.54$, which uses initial state (26). The linear dependence of the standard deviation with the time steps is a remarkable characteristic of the quantum walk which may be checked in actual physical implementations.

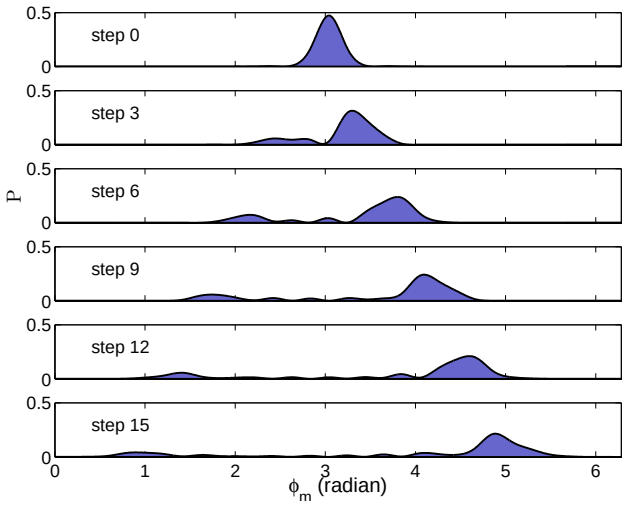

FIG. 2. (Color Online) The (unnormalized) phase probability distribution of the quantum walker after steps $l = 0, 3, \ldots, 15$. Here, the initial state (13) with $|\alpha_0| = 5$ has been used and the dimension of the Hilbert space has been set to $d = 31$.

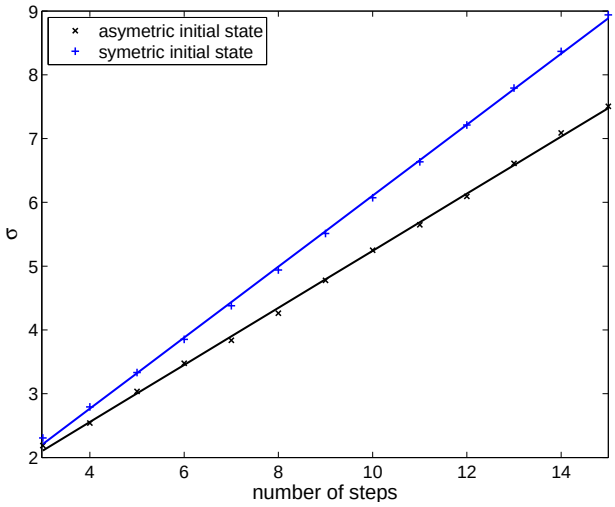

FIG. 3. (Color Online) The phase standard deviation as function of the number of steps for two initial states. The black line ($+$ points) uses state (13) and the blue line ($\times$ points) uses state (26) [compare with Figs. 2 and 4].

B. Normalizing the probability distribution

The areas under the plots depicted in Fig. 2 are not equal to one. This follows from the fact that state (22) has norm strictly smaller than one when d is finite. The tails of the series of the coherent states are lost when they are projected into Hilbert space H_d. Moreover, the area under the plot is changing during the evolution of the system, because there is a vertical displacement of the coherent state in the phase space produced by operator $e^{-i\tau\varepsilon(a^\dagger+a)}$, affecting α's [Eq. (18)] in each time step and consequently modifying the norm of $|\psi_l\rangle_d$.

For sufficiently small $\tau\varepsilon$, the norm of $|\psi_l\rangle_d$ does not depend on l and is almost equal to the norm of the truncated initial coherent state

$$\langle\alpha_0|\alpha_0\rangle_d = e^{-|\alpha|^2}\sum_{j=0}^{d-1}\frac{|\alpha|^{2j}}{j!}. \tag{25}$$

By setting $\varepsilon = 0$ and $\Delta = 0$ in the propagator, a standard quantum walk on a cycle would be obtained. To normalize $P^{(l)}(m)$, $|\psi_0\rangle_d$ should be normalized by dividing it by $|\langle\alpha_0|\alpha_0\rangle_d|$.

The effect of nonzero Δ when $\tau\varepsilon$ is sufficiently small is a free shift by angle $e^{i\tau\Delta}$ in each time step independently of the coin state. This term introduces a bias which can be clockwise or counterclockwise depending on the sign of Δ.

For large $\tau\varepsilon$ the position of the walker goes off the cycle destroying the ballistic dynamics of the walk. Therefore it is important to keep it small. Since $\tau = \pi/2\Omega_m$ and Ω_m ranges from KHz to GHz [24], it implies that ε can be sufficiently large and still the condition $\tau\varepsilon \ll 1$ is satisfied.

C. Symmetric probability distribution

The Hadamard-like transformation (10) treats coin states $|+\rangle$ and $|-\rangle$ in the same way and does not bias the walk [32]. Therefore starting the walk with the symmetric state $(1/\sqrt{2})(|+\rangle + |-\rangle)|\varphi_m\rangle$ leads to a symmetric distribution around φ_m. Starting the walk in a superposition of states $|\varphi_m\rangle$ (non-local state), so that each of them is symmetric, still produces a symmetric probability distribution if the amplitudes are real. However the truncated coherent state $|\alpha_0\rangle_d$ is a superposition of phase states with complex amplitudes. Distinct phase factors will interfere during the evolution destroying the symmetry.

The (unnormalized) probability distributions with the initial state

$$|\psi_0'\rangle = \frac{1}{\sqrt{2}}\Big(|+\rangle + |-\rangle\Big)|\alpha_0\rangle \tag{26}$$

are depicted in Fig. 4 for some values of l. It must be mentioned that with the initial state (26), Eqs. (16) is slightly modified. In this case, the walker evolves in a more symmetric way than the case with the initial state (13).

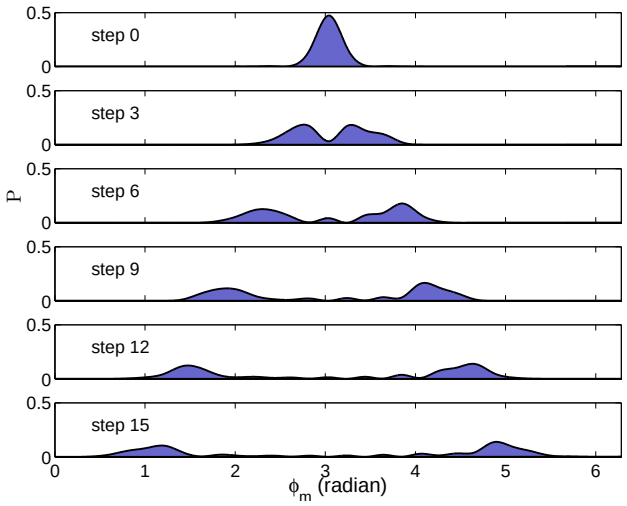

FIG. 4. (Color Online) The (unnormalized) phase probability distribution of the quantum walker after steps $l = 0, 3, \ldots, 15$. Here, the initial state (26) with $|\alpha_0| = 5$ has been used and the dimension of the Hilbert space has been set to $d = 31$.

III. DECOHERENCE

Both the optical and the mechanical resonator can be affected by noise. As we have discussed the dissipation effect on the optical field is counteracted by the driving so that it is left in an undepleted coherent state of amplitude $|\alpha| \propto \varepsilon/\gamma$, where γ is the relaxation constant for the amplitude damping channel (see for example [33]). However, the noise effects are more severe over the mechanical resonator, particularly in the situation where only two lowest levels are relevant. Therefore, the coherence time of this two-level resonator limits the total random walk evolution time. We consider the effect of the dephasing channel on the two-level resonator, or in terms of the quantum walk interpretation, we analyze a decoherent coin.

The unitary evolution of the quantum walk in each time step is driven by the unitary operator U given by Eq. (9). In the presence of imperfections the quantum walk evolution is not unitary and can be described by

$$\rho_l = \sum_j K_j U \rho_{l-1} U^\dagger K_j^\dagger, \tag{27}$$

where ρ_l is the density operator of the walker plus coin system and K_j are the Kraus operators modeling the quantum noise. The effect of the phase damping channel on the two-sided coin can be modeled by the Kraus operators $K_j = I_w \otimes E_j$, $j = 1, 2$ where I_w is the identity operator on the walker space and [34]

$$E_0 = \begin{pmatrix} 1 & 0 \\ 0 & \sqrt{1-\lambda} \end{pmatrix}, \qquad E_1 = \begin{pmatrix} 0 & 0 \\ 0 & \sqrt{\lambda} \end{pmatrix}. \tag{28}$$

where λ quantifies the strength of the channel and can be written as $\lambda = 1 - e^{-l\tau/T_d}$, being T_d the dephasing time. The amount of phase damping increases as time goes on.

Using the results of the previous section, the density operator of the system at step l is written as

$$\begin{aligned}\rho_l = \sum_{k,k'}\{\, & r^{(l)}_{2k-1,2k'-1}\,|+\rangle\langle+|\,|\alpha_{2k-1}\rangle\langle\alpha_{2k'-1}| \\ & + r^{(l)}_{2k-1,2k'}\,|+\rangle\langle-|\,|\alpha_{2k-1}\rangle\langle\alpha_{2k'}| \\ & + r^{(l)}_{2k,2k'-1}\,|-\rangle\langle+|\,|\alpha_{2k}\rangle\langle\alpha_{2k'-1}| \\ & + r^{(l)}_{2k,2k'}\,|-\rangle\langle-|\,|\alpha_{2k}\rangle\langle\alpha_{2k'}|\,\},\end{aligned} \tag{29}$$

where $1 \le l \le n$ and the coefficients r for $l \ge 2$are given by

$$\begin{cases} r^{(l)}_{2k-1,2k'-1} &= \frac{1}{2}\, r^{(l-1)}_{k,k'} \\ r^{(l)}_{2k-1,2k'} &= -\frac{i}{2}(-1)^k\, r^{(l-1)}_{k,k'} \\ r^{(l)}_{2k,2k'-1} &= \frac{i}{2}(-1)^k\, r^{(l-1)}_{k,k'} \\ r^{(l)}_{2k,2k'} &= \frac{1}{2}\, r^{(l-1)}_{k,k'}, \end{cases} \tag{30}$$

when k and k' have the same parity and

$$\begin{cases} r^{(l)}_{2k-1,2k'-1} &= -\frac{i}{2}(-1)^k\sqrt{1-\lambda}\, r^{(l-1)}_{k,k'} \\ r^{(l)}_{2k-1,2k'} &= \frac{1}{2}\sqrt{1-\lambda}\, r^{(l-1)}_{k,k'} \\ r^{(l)}_{2k,2k'-1} &= \frac{1}{2}\sqrt{1-\lambda}\, r^{(l-1)}_{k,k'} \\ r^{(l)}_{2k,2k'} &= \frac{i}{2}(-1)^k\sqrt{1-\lambda}\, r^{(l-1)}_{k,k'}, \end{cases} \tag{31}$$

when k and k' have different parities. The initial condition for the symmetric case is $r^{(1)}_{1,1} = r^{(1)}_{2,2} = 1/2$, and $r^{(1)}_{1,2} = r^{(1)}_{2,1} = \sqrt{1-\lambda}/2$.

The (unnormalized) probability distribution in the phase space is then calculated as

$$\begin{aligned} P^{(l)}(m) &= \langle+|\langle\varphi_m|\rho_l|\varphi_m\rangle|+\rangle \\ &+ \langle-|\langle\varphi_m|\rho_l|\varphi_m\rangle|-\rangle \\ &= \sum_{k,k'} r^{(l)}_{2k-1,2k'-1}\langle\alpha_{2k-1}|\varphi_m\rangle\langle\varphi_m|\alpha_{2k'-1}\rangle \\ &+ \sum_{k,k'} r^{(l)}_{2k,2k'}\langle\alpha_{2k}|\varphi_m\rangle\langle\varphi_m|\alpha_{2k'}\rangle\Big\}. \end{aligned} \tag{32}$$

Fig. 5 depicts $P^{(l)}(m)$ after $l = 9$ time steps for different values of dephasing time T_d. The figure shows the quantum-to-classical transition of the quantum walk dynamics when dephasing time decreases. Fig. 6 shows the phase standard deviation (σ) as a function of time steps (l) for different values of dephasing time T_d in the log-log scale. The black continuous line shows the linear dependence of σ with the number of steps in the perfect case $T_d = \infty$. The linear dependence of σ gradually converts to the curve $\sqrt{l}$ when the dephasing time decreases. The red continuous curve is $\sigma \propto \sqrt{l}$ and indicates that σ evolves proportional to the square root of time steps when decoherence is maximum. We see therefore a rapid degrading of the quantum feature on the walk for a dephasing time T_d smaller than tens of the time step τ. Collecting the parameters necessary for this implementation we know that on typical optomechanical experiments [24] the mechanical resonator frequency Ω_m ranges from KHz to GHz and therefore

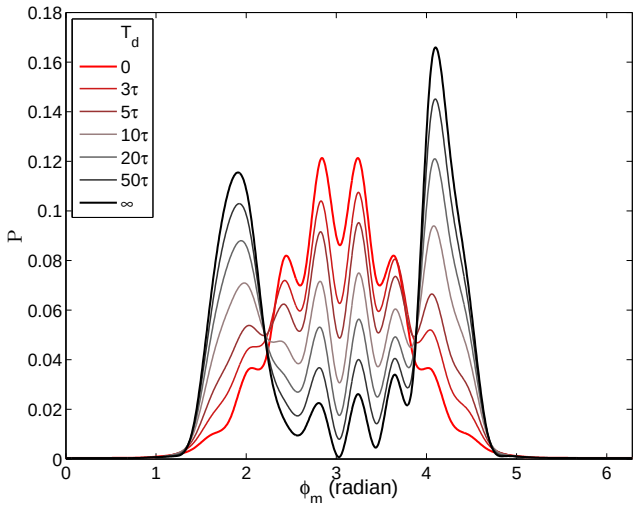

FIG. 5. (Color Online) The (unnormalized) phase probability distribution of the quantum walker after $l = 9$ steps for different values of dephasing time T_d. Here, the initial state (26) has been used.

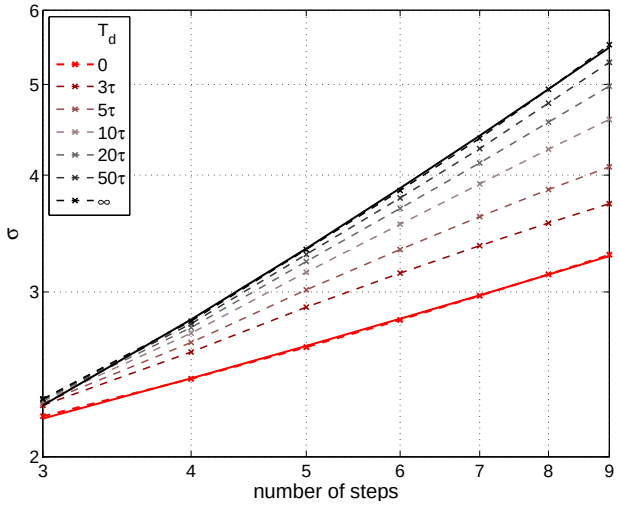

FIG. 6. (Color Online) The standard deviation of the walker in terms of the number of steps l for different values of dephasing time T_d in log-log scale [compare with Fig. 5].

the time step τ ranges from 10^{-3} to 10^{-9} s. Depending on the specific implementation the optical and mechanical relaxation rate may vary enormously. Particularly in the electromechanical system discussed in [28] $\Omega_m \approx 10^7$ Hz and $1/T_d \approx 10^1$ and therefore $T_d \approx 10^6\tau$ implying that the decoherence on the coin is almost negligible and so the quantum walk can be implemented over a large number of steps n. Similar conclusions are valid for the optomechanical system in [35].

IV. DISCUSSION

We have presented a proposal for implementation of a quantum walk on a circle using optomechanical systems. The walker is described by the coherent state in the phase space of the light field while the coin is encoded on the states of a mechanical resonator. We have ilustrated the process by considering the simplest case of a two-sided coin where only the two-lowest states of the mechanical resonator are relevant. The coherent state moves around a circle in the phase space so that the number of sites and its radius can be chosen by tuning the number of photons in the optical cavity. The number of sites in the cycle is limited by around 145. Despite that the total number of steps of the walker is not limited, but periodic in the cycle.

We have performed numerical simulations of the dynamics of the proposed scheme, which display the signatures of the discrete-time coined quantum walk on cycles. The ballistic behavior can be verified in two ways: (1) the probability distribution has two high peaks moving in opposite directions away from the origin, and (2) the standard deviation of the phase probability distribution is proportional to the number of steps. It is well known that classical random walks have a normal probability distribution and the standard deviation is proportional to the square root of the number of steps.

We have analyzed the decoherence effects over the coin by using the phase damping channel. We conclude that the decoherence time is large enough to allow the observation of the quantum behavior with present-day experimental parameters. As a last remark we should mention that for practical purposes the phase of the walker is easily detected through standard homodyne measurements, while the measurement of the population of the two lowest states of the mechanical resonator requires a more involved procedure. This is currently a subject of intense research and the details for that detection depends on the specific optomechanical or electromechanical implementation. In fact the experiments recently reported in Refs. [36, 37] open a new and promissing perspective.

We are currently extending the quantum walk model to analyze localization and to implement spatial search algorithms on two-dimensional lattices, by using two coupled optomechanical resonators—an aspect which shall be addressed elsewhere. We believe that physical realizations of quantum walks on optomechanical systems may bring practical applications quicker than the realization of a general-purpose quantum computer.

ACKNOWLEDGMENTS

JKM and RP acknowledge financial support from Faperj and CNPq. MCO acknowledges support from CNPq/FAPESP through the Instituto Nacional de Ciência e Tecnologia em Informação Quântica (INCT-IQ) and FAPESP through the Research Center in Optics and Photonics (CePOF).

[1] Y. Aharonov, L. Davidovich, and N. Zagury, Physical Review A **48**, 1687 (1993).
[2] R. Vieira, E. P. M. Amorim, and G. Rigolin, Physical Review Letters **111**, 180503 (2013).
[3] A. M. Childs, R. Cleve, E. Deotto, E. Farhi, S. Gutmann, and D. a. Spielman, Proceedings of the thirty-fifth ACM symposium on Theory of computing - STOC '03 , 59 (2003).
[4] A. Childs and J. Goldstone, Physical Review A **70**, 1 (2004).
[5] R. Portugal, Quantum Walks and Search Algorithms (Springer, New York, NY, 2013).
[6] K. Manouchehri and J. Wang, Physical Implementation of Quantum Walks (Springer, Berlin, Heidelberg, 2014).
[7] D. Bouwmeester, I. Marzoli, G. Karman, W. Schleich, and J. Woerdman, Physical Review A **61**, 013410 (1999).
[8] P. Souto Ribeiro, S. Walborn, C. Raitz, L. Davidovich, and N. Zagury, Physical Review A **78**, 012326 (2008).
[9] M. A. Broome, A. Fedrizzi, B. P. Lanyon, I. Kassal, A. Aspuru-Guzik, and A. G. White, Physical Review Letters **104**, 153602 (2010).
[10] P. Zhang, B.-H. Liu, R.-F. Liu, H.-R. Li, F.-L. Li, and G.-C. Guo, Physical Review A **81**, 052322 (2010).
[11] A. Peruzzo, M. Lobino, J. C. F. Matthews, N. Matsuda, A. Politi, K. Poulios, X.-Q. Zhou, Y. Lahini, N. Ismail, K. Wörhoff, Y. Bromberg, Y. Silberberg, M. G. Thompson, and J. L. OBrien, Science (New York, N.Y.) **329**, 1500 (2010).
[12] A. Schreiber, K. N. Cassemiro, V. Potoček, A. Gábris, P. J. Mosley, E. Andersson, I. Jex, and C. Silberhorn, Physical Review Letters **104**, 050502 (2010).
[13] A. Schreiber, K. N. Cassemiro, V. Potoček, A. Gábris, I. Jex, and C. Silberhorn, Physical Review Letters **106**, 180403 (2011).
[14] S. K. Goyal, F. S. Roux, A. Forbes, and T. Konrad, Physical Review Letters **110**, 263602 (2013).
[15] P. Xue, B. Sanders, and D. Leibfried, Physical Review Letters **103**, 183602 (2009).
[16] M. Karski, L. Förster, J.-M. Choi, A. Steffen, W. Alt, D. Meschede, and A. Widera, Science (New York, N.Y.) **325**, 174 (2009).
[17] F. Zähringer, G. Kirchmair, R. Gerritsma, E. Solano, R. Blatt, and C. F. Roos, Physical Review Letters **104**, 100503 (2010).
[18] H. Schmitz, R. Matjeschk, C. Schneider, J. Glueckert, M. Enderlein, T. Huber, and T. Schaetz, Physical Review Letters **103**, 090504 (2009).
[19] W. Dür, R. Raussendorf, V. Kendon, and H.-J. Briegel, Physical Review A **66**, 052319 (2002).
[20] B. Travaglione and G. Milburn, Physical Review A **65**, 032310 (2002).
[21] B. C. Sanders, S. D. Bartlett, B. Tregenna, and P. L. Knight, Physical Review A **67**, 042305 (2003).
[22] P. Xue and B. C. Sanders, New Journal of Physics **10**, 053025 (2008).
[23] P. Xue, B. Sanders, A. Blais, and K. Lalumière, Physical Review A **78**, 042334 (2008).
[24] M. Aspelmeyer, T. J. Kippenberg, and F. Marquardt, arXiv:1303.0733 (2013).
[25] M. Poot and H. S. van der Zant, Physics Reports **511**, 273 (2012), mechanical systems in the quantum regime.

[26] A. D. O'Connell, M. Hofheinz, M. Ansmann, R. C. Bialczak, M. Lenander, E. Lucero, M. Neeley, D. Sank, H. Wang, M. Weides, et al., Nature **464**, 697 (2010).
[27] J. Chan, T. P. M. Alegre, A. H. Safavi-Naeini, J. T. Hill, A. Krause, S. Gröblacher, M. Aspelmeyer, and O. Painter, Nature **478**, 89 (2011).
[28] J. D. Teufel, T. Donner, M. A. Castellanos-Beltran, J. W. Harlow, and K. W. Lehnert, Nature nanotechnology **4**, 820 (2009).
[29] M. Suzuki, Journal of mathematical physics **26**, 601 (1985).
[30] M. Suzuki, Communications in Mathematical Physics **51**, 183 (1976).
[31] R. Loudon, The quantum theory of light (Oxford university press, 2000).
[32] J. Kempe, Contemporary Physics **44**, 302 (2003), quant-ph/0303081.
[33] M. C. de Oliveira, M. H. Y. Moussa, and S. S. Mizrahi, Phys. Rev. A **61**, 063809 (2000).
[34] M. A. Nielsen and I. L. Chuang, (Cambridge university press, New York, 2010).
[35] E. Verhagen, S. Deleglise, S. Weis, A. Schliesser, and T. J. Kippenberg, Nature **482**, 63 (2012).
[36] H. Okamoto, A. Gourgout, C.-Y. Chang, K. Onomitsu, I. Mahboob, E. Y. Chang, and H. Yamaguchi, Nature Physics **9**, 480 (2013).
[37] T. Faust, J. Rieger, M. Seitner, J. Kotthaus, and E. Weig, Nature Physics **9**, 485 (2013).